DOI: 10.1021/ma1000282

Macromolecules
ARTICLE

Deformation-Induced Phase Transitions of Polyamide 12 at Different Temperatures: An in Situ Wide-Angle X-ray Scattering Study

Daoliang Wang,[†] Chunguang Shao,[†] Baijin Zhao,[†] Liangui Bai,[†] Xiao Wang,[†] Tingzi Yan,[†] Junjun Li,[†] Guoqiang Pan,[†] and Liangbin Li*[,†,‡]

[†]*National Synchrotron Radiation Lab and College of Nuclear Science and Technology, University of Science and Technology of China, Hefei, China, and* [‡]*CAS Key Lab of Soft Matter Chemistry, University of Science and Technology of China, Hefei, China*

Received September 14, 2009

ABSTRACT: Deformation-induced phase transition of polyamide 12 (PA 12) was studied with in situ wide-angle X-ray scattering (WAXS) at temperatures below and above glass transition temperature. Irrespective to the testing temperature, a transient α″ phase occurred in the early plastic deformation stage, whose lifetime is decreasing with the increase of temperature. At temperature below glass transition temperature, the transient α″ phase further transforms into a mesomorphic state with increasing the strain, while high temperature promotes the transient α″ phase transforming into γ′ phase. The different final states at temperatures below and above glass transition temperature is due to the competition and coupling between external work and thermal activation. External work from tensile deformation is responsible for the appearance of the transient α″ phase and the final mesomorphic state at temperature below glass transition temperature, while thermal activation drives the transition from the transient α″ phase to γ′ phase. All these phase transitions occur in the plastic deformation region, which shows a close correlation between the mechanical response and the structural evolution during tensile deformation.

Introduction

Deformation-induced structural formation and evolution of polymers stands at the important position in polymer science and industry, as polymer is subjected substantially mechanical deformation during processing as well as in actual application. For example, fiber spinning is a solidification process under strong deformation, during which either liquid−solid or solid−solid phase transitions may take place.[1,2] On the other hand, crystal−crystal transition during mechanical test can also leads to unique mechanical properties. A good example is the superelasticity of sydiotactic polypropylene (sPP), where a stress-induced martensitic-like crystal−crystal phase transition occurs and provides such a unique mechanical behavior.[3]

Deformation-induced phase transition is a rather complicated process.[4−6] A multistage process has been observed in many polymer systems, where a transient phase occurs to assist the transition from the initial to the final phases. Drawing supercooled polyethylene (PE) melt may induce the conformational disordered hexagonal crystal (Condis) first, which subsequently transforms into stable orthorhombic one.[7] Deformation-induced mesophases are widely observed in semirigid chain polymers like polyethylene terephthalate (PET) and polyethylene nathphalate (PEN) during drawing around glass transition temperatures.[8−16]

Deformation-induced crystal−crystal phase transitions are a common behavior of polyamide family like PA 6[17−19] and PA 12.[20−22] PA 12 possesses four different crystal forms, namely γ, γ′, α, and α′.[21,23−25] γ form is the most common and easy to be obtained one with a hexagonal or sometime pseudohexagonal packing,[28] which is characterized with a strong diffraction peak with a spacing around 0.41−0.42 nm. The structure of the γ′ form is similar to the γ form, which can be distinguished through the capability of transition to α form[21] or by solid NMR measurements.[23,26] A deformation-induced γ−γ′ crystal−crystal transition has been reported in PA 12, by drawing above 50 °C at atmospheric pressure.[21] while at temperature close to melting point γ−α phase transition takes place under drawing.[20,22] The transition processes among these phases are still not fully understood, which requires the aid of in situ techniques like X-ray scattering.

In this work, an in situ wide-angle X-ray scattering (WAXS) measurements are performed to monitor phase transitions of PA 12 during uniaxial tensile deformation at different temperatures. A transient phase was observed during the transition, whose lifetime is decreasing with the increase of temperature. The final structure is determined by the competition and coupling between stimulations from thermal activation and external work, which can be either a mesomorphic structure at room temperature or γ′ crystal at high temperatures. The existence of transient phase may have some implication on drawing ability of PA 12 in industry processing.

Experimental Section

Material and Sample Preparation. PA 12 granules are supplied by Evonik Degussa with a trade name of L1600. The melting point and glass transition temperature are about 178 and 40 °C, respectively. PA 12 plates with a thickness about 1 mm were obtained by compression molding, which were dried at 60 °C for 12 h in vacuum to eliminate moisture. For tensile test, isothermally crystallized plates were used, which were crystallized at 140 °C for 2 h in nitrogen atmosphere after melting the plates at 210 °C. Finally, the plates were cut into dumbbell shape, with length and width of 29 and 4 mm, respectively, for uniaxial tensile deformation.

In Situ Synchrotron Wide-Angle X-ray Scattering Measurement. A homemade miniature mechanical tester was employed

*Correspondence author. E-mail: lbli@ustc.edu.cn.

 Published on Web 02/12/2010 © 2010 American Chemical Society

to carry out the tensile test, which is equipped with temperature controlled oven with nitrogen purge. The mechanical error of the apparatus is less than 0.02 mm with a stretching range of 100 mm. Error of the force sensor is less than 1 N. In this work, the uniaxial tensile tests were performed at several designated temperatures and the stretching rate was fixed at 1.165 μm/s.

In situ WAXS measurements were carried out on the synchrotron radiation X-ray scattering station with a radiation wavelength of 0.154 nm and Mar 345 image plate as a detector in National Synchrotron Radiation Laboratory (NSRL) in Hefei (China). Fit2D software package was used to analyze the two-dimensional (2D) WAXS patterns. Air background was deducted and then the total intensity was normalized. The diffraction peak position, intensity, and full width at half-maximum (fwhm) were extracted through Gaussian peak fitting.

DSC, IR, and Raman Test. Differential scanning calorimetry (DSC) thermograms of undeformed and deformed samples were measured from 25 to 230 °C with a heating rate of 10 and 90 °C/min on Shimadzu DSC-60 instrument.

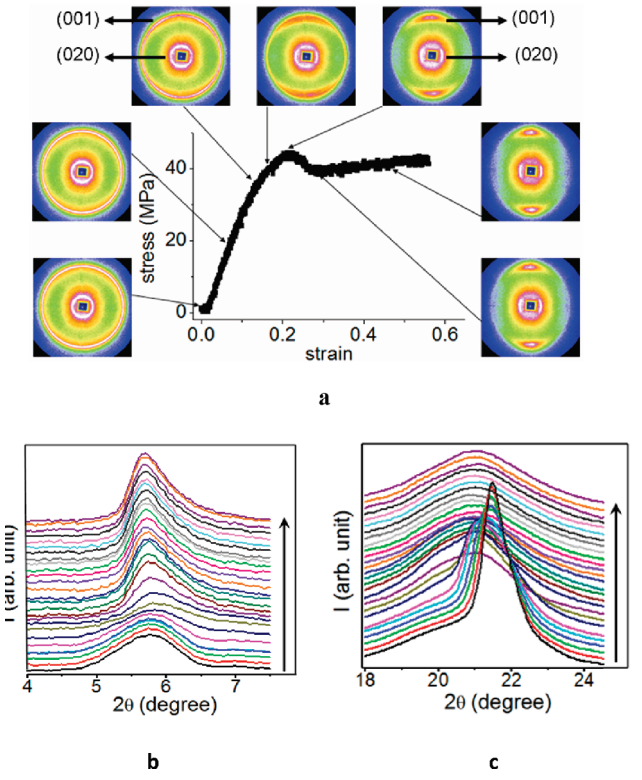

Figure 1. Engineering stress−strain curve and the selected WAXS patterns during uniaxial tensile deformation at room temperature (a) (the tensile axis is along the horizontal direction), and the corresponding 1D WAXS curves for (b) (020) and (c) (001) peaks (The arrow indicates increase of strain).

Fourier transformation infrared (FTIR) absorption spectra of undeformed and deformed samples were measured between 400 and 4000 cm^{-1} using a Nicolet 8700 instrument. The thin films with a thickness of about 100 μm were prepared with a microtome.

Laser Raman spectra were obtained between 400 and 4000 cm^{-1} using a LABRAM-HR (JY, France) laser Raman Spectroscope equipped with a microscope. The excitation wavelength was 514.5 nm with a argon ion laser.

Results

The γ phase is the most stable form for PA 12 crystal at room temperature. According to the crystallization condition adopted in this work, the crystal phase in the PA 12 samples before tensile test was γ phase, which was verified by the WAXS pattern. For the undeformed samples, there are two main diffraction peaks in WAXS curves which belong to the γ phase of PA 12. One is (001) at 2θ of 21.5° and the other one is (020) at 2θ of 5.8° (*b*-axis is the chain axis).

Figure 1a shows the engineering stress−strain curve during tensile test at room temperature (25 °C controlled by air condition), where selected 2D WAXS patterns at various strain levels are inserted. The tensile direction is along the horizontal direction. The development of stretching induced orientation of crystals can be easily visualized while the small shift of peak position requires a detailed analysis of the integrated one-dimensional (1D) WAXS curves. The integrated 1D WAXS curves during the stretching process at room temperature are shown in Figure 1, parts b and c, which correspond to the scattering of (020) and (001) planes, respectively. With applied strain, significant shift of peak position is observed for both (020) and (001) peaks. A peculiar feature is also observed for (020) peak, whose position first shifts to large angle direction and switches back to the low angle side during tensile test. Accompanied with this process, the peak intensity also shows a minimum point. In order to have a close look at the evolution of peak position during tensile deformation, Figure 2, parts a and b, plot the *d* spacings of (020) and (001), respectively, which are obtained through Gaussian peak fitting. To avoid possible artifact during peak fitting, we only fit one crystalline and one amorphous peak for the WAXS peak around (001) position, though this peak may contain multiple diffraction peaks as presented in Figure 4. The engineering stress−strain curve is also plotted in the same figure for a direct comparison. The evolutions of *d* spacings of both (001) and (020) planes can be divided into three stages, which are labeled with red dash lines and indicated as zone I, II, and III, respectively. In zone I, the *d* spacing of (001) plane increases with strains nearly propositionally, while the *d* spacing of (020) plane shows a small reduction. Zone I matches well with the linear deformation region as indicated by the stress−strain curve. Upon the stress−strain curve deviating from the linear deformation behavior (we denoted this point as the first yield point and the starting of zone II),

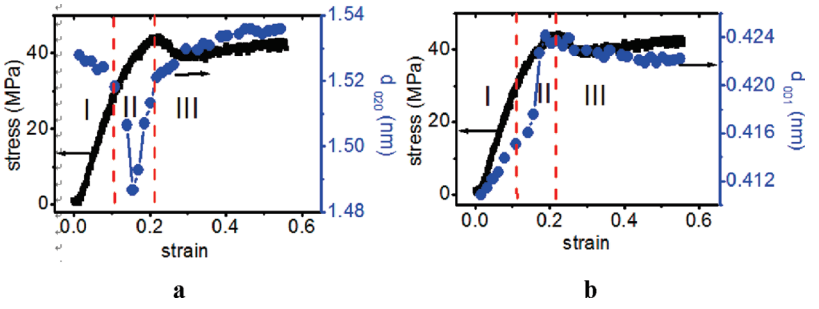

Figure 2. Change of *d* spacing of (a) (020) plane and (b) (001) plane by WAXS in conjunction with engineering stress−strain curve during uniaxial deformation at room temperature.

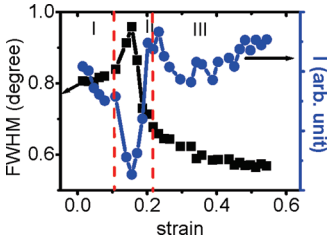

Figure 3. Fwhm and intensity of (020) peak as a function of strain.

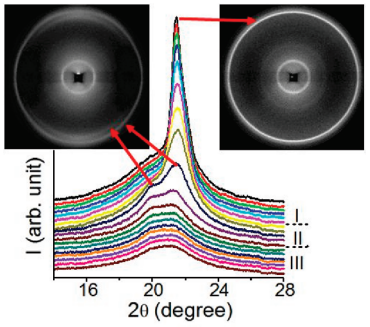

Figure 4. Diffraction intensity of (001) collected from vertical scans and selected 2D WAXS patterns during tensile deformation at room temperature.

the *d* spacings of (001) and (020) show sharp jumps where (001) increases and (020) decreases. The *d* spacing of (001) reaches a plateau, while the *d* spacing of (020) goes to a minimum and increases again sharply. The increase of (020) *d* spacing slows down after the second yield point in the stress−strain curve, which is the transitional point from zone II to zone III. Two remarkable points need to be stressed here. (i) The transition points of these three zones of *d* spacing match well with the stress−strain curve at the first and the second yield points. This indicates a correlation between the mechanical properties and the structural transitions. (ii) The evolution of (020) *d* spacing is nonmonotonic and has a minimum with strain. This suggests that the transition from the initial structure to the final structure may undergo a transient phase. If the transition from initial γ phase to the final state follows a direct process, one would expect the evolution of *d* spacing goes a monotonic fashion.

The nonmonotonic evolution during tensile deformation is also reflected from the intensity and fwhm of (020) reflection, which is plotted with strain in Figure 3. Similar with that in Figure 2, both the intensity and fwhm have a sharp jump in zone II. The intensity goes to a minimum and then increases sharply, while the fwhm of (020) peak reaches to a maximum and then decreases fast, which suggest that a transient phase may occur. In zone III, fwhm reaches a plateau which is even smaller than that in zone I. Meanwhile, the intensity also comes to a plateau, which is slightly higher than that in zone I. In the final deformed sample the smaller fwhm of (020) indicates the increase of correlation length or size of crystal along chain axis direction, while slightly higher intensity suggests the increase of volume fraction of such a structure.

The existence of the transient phase is further confirmed by a detailed analysis of the diffraction in the vertical direction. As shown in Figure 4 of the 2D and 1D WAXS patterns, in zone II a new diffraction peak shows up at lower angle near (001) peak in the vertical direction, which locates around the peak position of the amorphous halo. Upon a further increase in the strain, the signal of this new peak disappears gradually and a broad single peak exists at the end of the stretching. At the final state, a combination of the sharp diffraction peak of (020) and the broad diffraction peak around initial (001) position exist. The difference

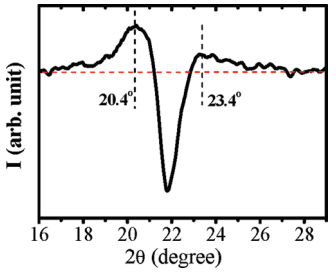

Figure 5. Difference curve during tensile deformation at room temperature.

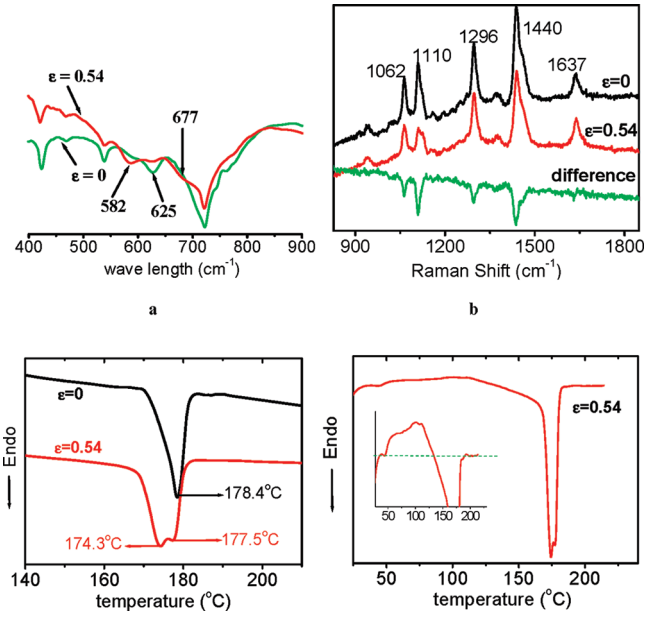

Figure 6. IR spectra (a), Raman spectra (b), and DSC curve (c, d) of undeformed and deformed PA 12 samples (drawing at room temperature).

WAXS curve at strain ε of 0.15 (in zone II) is shown in Figure 5, which makes the new peaks more visible. Two peaks instead of one located at 2θ of 20.4 (d = 0.435 nm) and 23.4 (d = 0.379 nm) are identified, which are close to the diffraction of α phase of PA 12. As γ phase has a small peak around 23°, the difference curve in Figure 5 gives the second peak at 23.4° rather weak. The identification of the second peak at 23.4° is supported by another work from our group, where PA 12 copolymers is studied and two diffraction peaks can be directly observed without any data treatment.[44] We can not directly assign this deformation-induced phase as α crystal because α crystal in PA 12 forms under deformation at temperatures close to melting point of PA 12. For convenience, the new phase is denoted as α″ phase.[44]

Figure 6a shows the IR spectra of deformed (ε = 0.54) and undeformed samples (ε = 0). The absorption band (shoulder peak) at 677 cm^{-1} (amide V (α); C═O out-of-plane bend) is observed in deformed sample, and the decrease of 625 cm^{-1} (amide VI (γ); N−H out-of-plane bend) is accompanied by the increase of 582 cm^{-1} (amide VI (α); N−H out-of-plane bend),[22,45] indicating that the structure in the final deformed state has a similar conformation with that of α form of PA 12. In another word, tensile deformation may transform the H-bonds between parallel chains (γ form) to antiparallel chains (α form), which will be described in following discussion part.

Figure 6b depicts the Raman spectra of undeformed sample (ε = 0), deformed sample (ε = 0.54) and their difference. The amide I (1637 cm^{-1}) is attributed to the C═O stretch, which is

taken as the reference. The 1110 and 1062 cm^{-1}(C−C stretch) peaks and the 1296 cm^{-1} (CH_2 twisting) peak are indicative of an all-trans C−C backbone conformation.[46−48] They both decrease after tensile deformation, which demonstrate the reduction of all-trans C−C conformation in the deformed sample. Another significant change after deformation is the decrease of the peak intensity at 1440 cm^{-1} (CH_2 bending), which can be used as a measure of chain−chain coupling analogous to the case of polyethylene (PE).[47,49] The decrease of peak intensity at 1440 cm^{-1} indicates the reduction of the degree of inter chain order in the final deformed sample.

Figure 6c gives the DSC data of the deformed (ε = 0.54) and undeformed samples (The heating rate is 10 °C/min.). Before tensile deformation PA 12 film has one melting peak at178.4 °C, while the deformed samples give two melting peaks at 174.3 and 177.5 °C, respectively. Figure 6d gives the full view of DSC curve for deformed sample, in which the partially enlarged view is inserted in the left. From the inserted figure, one can easily find that there is a slow recrystallization process in wide temperature range, which indicates a unstable state exists in the deformed sample. In order to confirm the recrystallization phenomena of deformed sample, we also carry out a reference DSC experiment with a fast heating rate of 90 °C/min and no obvious recrystallization peak can be revealed.

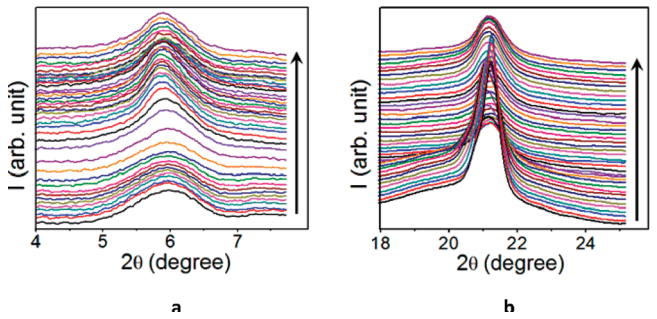

Figure 7. Progress of 1D WAXS patterns for (a) (020) peak and (b) (001) peak during deformation at 120 °C (The right arrow indicates increase of strain).

In the final state after stretching, the transient phase does not transform into γ' phase at room temperature, which is similar to other early reports. The increase of intensity and the decrease of width of (020) diffraction peak in zone III indicate an ordering process in chain axis direction. However, a completely opposite evolution was taking place on (001) peak, which suggests a disordering process in interchain packing. Combining the WAXS, IR, Raman, and DSC data of PA 12 before and after tensile deformation at room temperature, the final state after tensile deformation is a structure with long-range order in chain axis direction but with conformational defects and reduction of inter chain order.

Similar behaviors are also found when the samples are stretched at temperatures above the glass transition temperature. For conciseness, we only present 1D WAXS curves for sample drawn at 120 °C (Figure 7). Comparing with that at room temperature, the change of diffraction peak for both (001) and (020) seems milder when stretching at high temperatures. The evolution of *d* spacing of (001) and (020) planes are plotted in conjunction with the engineering stress−strain curve, as shown in Figures 8, 9 and 10 for stretching at 60, 100, and 120 °C, respectively. Similar with that at room temperature, the large variation of the (020) *d* spacing also takes place in zone II for all tensile test at different temperatures. With applied strain in zone II, the *d* spacing of (020) plane goes to a minimum and increases again. However, with the increase of temperature, the transitional process of (020) *d* spacing in zone II is accelerated, which reduces the variation range of *d* spacing. Meanwhile, the new diffraction peak, indicating the transient phase as shown in Figure 4 is also weakening with the increase of temperature. The similar evolution trend of the (020) *d* spacing during tensile test at different temperatures further confirms the existence of the transient phase, though its lifetime is reduced by thermal activation at high temperatures.

The evolutions of the (001) *d* spacing are rather complicated during tensile deformation at different temperatures. At high

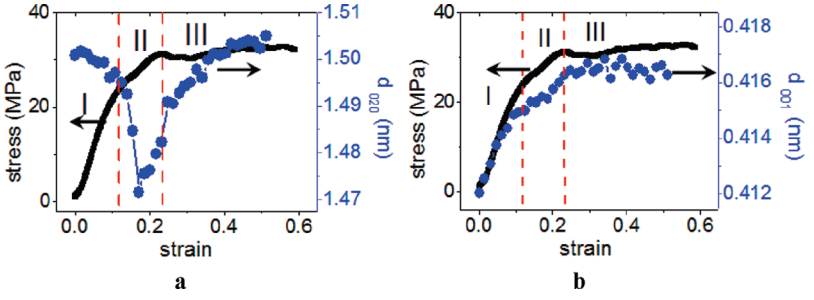

Figure 8. Change of *d* spacing of (a) (020) plane and (b) (001) plane by WAXS in conjunction with engineering stress−strain curve during uniaxial deformation at 60 °C.

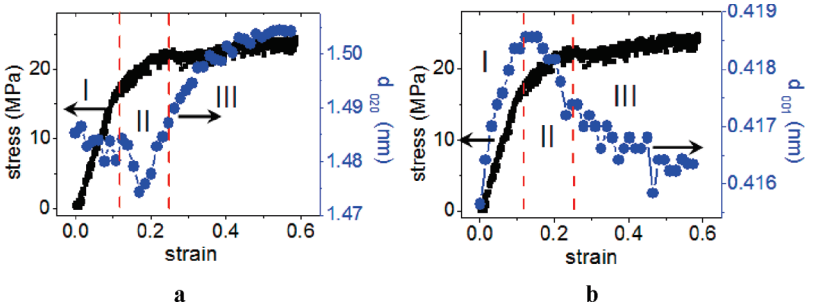

Figure 9. Change of *d* spacing of (a) (020) plane and (b) (001) plane by WAXS in conjunction with engineering stress−strain curve during uniaxial deformation at 100 °C.

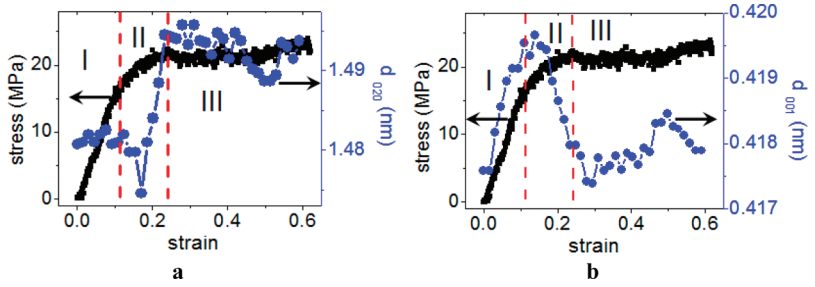

Figure 10. Change of *d* spacing of (a) (020) plane and (b) (001) plane by WAXS in conjunction with engineering stress−strain curve during uniaxial deformation at 120 °C.

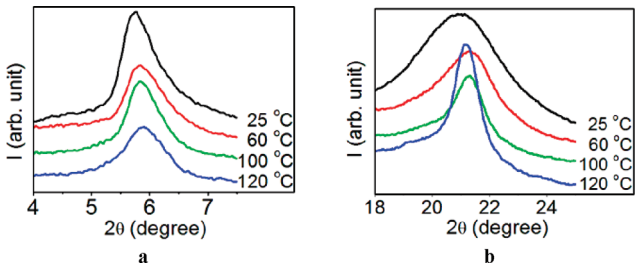

Figure 11. 1D WAXS patterns of samples after uniaxial deformation at indicated temperatures (a) for (020) peak and (b) for (001) peak.

temperatures, the *d* spacing of (001) plane increases with strain nearly propositionally in zone I, which is similar to that during drawing at room temperature. The sharp change of structure is still concentrated in zone II, which is typically termed as the beginning of plastic deformation stage. In Figures 8, 9, and 10, It is seen that the sharp change of (001) *d* spacing is always taking place in zone II at high temperatures, as the same as at room temperature. However, at high temperature the evolution trend of (001) *d* spacing is different from that at room temperature. At room temperature, the *d* spacing of (001) plane shows a sharp increase in zone II, whereas it slows down the increase at 60 °C, and the increase even switches to a decrease at 100 and 120 °C.

Comparing the *d* spacings of (001) and (020) before and after the tensile deformation, different variations occur at different temperatures. At room temperature and 60 °C, the *d* spacing of (001) increased after drawing, while the *d* spacing of (020) is nearly the same before and after drawing, though it runs through a minimum. At higher temperature, the trend seems completely different. The *d* spacing of (020) after drawing is larger than that of the initial sample, while the *d* spacing of (001) plane returns back to its initial value after reaching a maximum. In addition to these, the diffraction peak shape of the final state after drawing is also varied with temperature, which is mainly manifested in the (001) peaks as shown in Figure 11. With the increase of temperature, the (001) peak becomes sharper and sharper, which indicates that different phases are involved in final state (see Discussion).

Discussion

On the basis of the above results, several important facts can be extracted. (i) In WAXS measurements, the existence of the transient α″ phase can be clearly observed through the appearance of the two new diffraction peak when PA 12 samples is drawn into zone II at room temperature (see Figure 4). These peaks are weakening with the increase of temperature. (ii) If we employ the appearance of the minimum of (020) *d* spacing during drawing as the mark of the transient α″ phase, the lifetime as well as the amount of transient phase decreases with the increase of temperature. (iii) The abrupt changes of *d* spacing for both (001) and (020) are always observed in zone II, which is the onset of plastic deformation stage. This fact implies that there is a close connection between structural evolution and mechanical response under uniaxial tensile deformation.

It is clear that the transient α″ phase assists the transition from initial γ phase to the final phase during drawing at all temperatures we studied. It is well-known that γ form is the most stable crystal phase for PA 12. The γ form adopts a hexagonal or pseudohexagonal packing.[27−29] Comparing with the α form whose H-bonds are formed between antiparallel chains, the γ form involves H-bonds which are constructed between parallel chains and adopts a pseudohexagonal packing. As the main characteristic of polyamide, the H-bonds can be formed between adjacent chains with various conformations, which may result in metastable phases of polyamide under different states. Upon drawing into zone II, the external stress induces a transient phase which is similar to PA 12 α form. Take drawing at room temperature for example, two new diffraction peaks which are located at 20.4 and 23.4° respectively show up in zone II. Meanwhile the fwhm and intensity of (020) peak (indicates the periodicity along chain axis) increases and decreases, respectively, which indicate the degree of order along chain axis becomes weaker. This suggests that a transient phase α″ is induced by tensile deformation, which is a metastable phase and has no defined melting point as also supported by our another work.[44]

In the case of γ form, the extended CH_2 zigzags of each chain are in the plane of a molecular sheet, while the amide groups point in an angel about 60° out of the molecular sheet. Here the H-bonds connect parallel chains in adjacent molecular sheet. On the other hand, in the α type of structure, the H-bonds are constructed in the each molecular sheet between antiparallel chains. The transition from γ to α″ form involves the amide groups and results in an about 60° twist of H-bonds.[28] It is important to note that the transient α″ phase is always happening in zone II (the early stage of plastic deformation), the transition from γ to α″ form is probably due to the martensitic transformation induced by stress. It is well-known that the stress-induced martensitic transformation corresponds to the conversion of orthorhombic to monoclinic phase in polyethylene (PE), and the transformation is favored by lower temperature and higher crystallinities where stress are higher.[38,39] In this work, tensile deformation-induced transition from γ to α″ form is analogous to the martensitic transformation in PE; however, the α″ form is a metastable phase which will transform to other phase rapidly during tensile deformation.

In zone III, the final state during tensile deformation at room temperature (below T_g of PA 12) is a broad scattering halo observed in WAXS. The broad peak is mainly due to following possible reasons: the breaking of crystals or formation of a mesomorphic state. The crystal size becomes larger along the chain axis and much smaller perpendicular to the chain axis (estimate from the fwhm of 020 and 001 according to Scherrer formula), which means they are possibly the microfibrilar crystals after tensile deformation. However, base on the direct *d* spacing

data, the final state of crystal after tensile deformation does not pack closely, which suggests that the final state is a low density state like conformational disordered crystal or more generally a mesomorphic state. This is also supported by the reduction of C−C trans conformation measured on the deformed samples with Raman, the appearance of band at 667 cm^{-1} and the loss of band at 625 cm^{-1} in IR, and the recrystallization process during heating in DSC. The weakening of 1440 cm^{-1} in Raman also suggests the reduction of inter chain interaction, which is consistent with WAXS data. Combining WAXS result with the IR, Raman and DSC data, one can find that tensile deformation not only result in the fragmentation of lamella, but also lead to a modification of intra chain conformation and inter chain interaction. At this moment we tentatively call the final state as mesomorphic state and direct experimental data are required to clarify its structure, which may take much more effort like that on the mesophase of iPP.[50]

The transformation process is strongly depended on temperature, as the phase transition is activated by both external tensile stress and temperature.[30] At temperature lower than the glass transition temperature (about 40 °C), the effect of thermal excitation is minor, while the external work provided by the tensile deformation plays the major role to promote the phase transition. At temperatures well above the glass transition temperature, the role of thermal excitation slowly overwhelms the effect of external work. Evidently the external work from the tensile deformation is directly responsible to the appearance of the transient α'' phase. Below the glass transition temperature, tensile deformation induces the formation of the transient α'' phase, which further transforms into final state after large deformation due to lacking of sufficient thermal activation energy to promote it transforming into γ' phase. According to other report, tensile deformation induced $\gamma-\gamma'$ phase transition of PA 12 by drawing above 50 °C at atmospheric pressure.[21] γ' phase has a similar structure with γ phase (they cannot be distinguished by WAXS pattern), which can transform to α phase through thermal treatment under pressure. The same thermal treatment does not transform γ form into α crystal. The transition from the transient α'' phase to γ' phase should be mainly attributed to thermal activation under stress. With increasing temperature, the lifetime and amount of the transient phase decrease during tensile deformation.

It is also important to note that the abrupt changes of *d* spacing for both (001) and (020) are always happening in the early plastic deformation stage, which demonstrates the close connection between the physical structures and mechanical properties. The onset of plastic deformation indicates that some irreversible deformations occur. It is well-known that many complicated deformational behaviors are involved in the plastic deformation stage.[31−35] As far as the crystallographic deformation is concerned, the polymer crystal can deform plastically by slip, twinning and martensitic transformations.[31,36−39] Generally for double yield behavior of semicrystalline polymer, the first yield point is associated with the fine chain slip combined with a martensitic type of transformation within the lamella, whereas the second yield point is related to the coarse chain slip which will lead to lamella fragmentation.[40−43] Thus, in this work, in the early plastic deformation stage (zone II), polymer crystal may not be destroyed. We note that the transient α'' phase is always being produced and accompanied by the decrease of (020) *d* spacing (it represents the periodic distance along the chain axis) in zone II. This indicates that the first yield behavior is related to the appearance of α'' phase which may be caused by the martensitic transformation of γ crystal discussed above. Soon, the transient α'' phase is able to transform into the γ' phase at high temperature (or mesomorphic state at low temperature), which is reflected by the recovery of (020) and (001) *d* spacing in zone II as well. The transformation from γ phase to α'' phase and further to γ' phase (or mesomorphic state) in zone II is a continuous process. As the applied strain is up to the second yield point, the (020) *d* spacing will reach an equilibrium value. This is understandable because the fragmentation of crystal lamella begin to dominate the deformation of crystal thereafter. In another word, the *d* spacings of crystal will not change after the second yield point if no thermal stimulated phase transition proceeds. It is emphasized that the various phases (γ, α'', γ' and mesomorphic state) may coexist during the whole process of tensile deformation once they are generated. Additionally, although the yield behavior of crystalline polymer may be resulted in by various deformations of both crystal and amorphous region, it is no doubt that the yield behavior of PA 12 has a strong correlation with the phase transition processes. The macroscopic mechanical properties in the plastic deformation stage or zone II are the manifesting of phase transitions at molecular scale.

Conclusion

In situ wide-angle X-ray scattering (WAXS) was employed to monitor the phase transition of PA 12 during tensile deformation at different temperatures. At all temperatures (25, 60, 100, and 120 °C) we studied, a transient α'' phase occurs in the early plastic deformation stage, whose role is weakening with the increase of temperature. Determined by temperature, the transient phase transforms into either another mesomorphic structure at room temperature or γ' at temperatures above the glass transition temperature. The different phase transition kinetics as well as different final structures at different temperatures is attributed to the coupling and competition between thermal activation and external work provided by tensile deformation. Tensile deformation is responsible to the appearance of the transient α'' phase as well as the final mesomorphic state at room temperature, while thermal activation promotes the transition from the transient phase to γ' phase. The transient α'' phase always shows up in the early plastic deformation stage, which indicates that the transient phase has a close connection with the yield behavior. Our experimental results indicate that the macroscopic mechanical response correlates directly with phase transition at molecular level under uniaxial tensile deformation.

Acknowledgment. This work is supported by the NNSFC (20774091), Fund for one hundred talent scientist of CAS, the "NCET" program of MOE, 973 program of MOST and the experimental fund of NSRL. L.B.L. would like to thank Dr Zhidong Chen (Degussa) for providing Nylon-12 sample.

References and Notes

(1) Schultz, J. M.; Hsiao, B. S.; Samon, J. M. *Polymer* **2000**, *41*, 8887–8895.
(2) Samon, J. M.; Schultz, J. M.; Jing, Wu; Hsiao, B. S.; Fengji, Yeh; Kolb, R. *J. Polym. Sci., Part B: Polym. Phys.* **1999**, *37*, 1277–1287.
(3) Auriemma, F.; De Rosa, C.; Esposito, S.; Mitchell, G. R. *Angew. Chem., Int. Ed.* **2007**, *46*, 4325–4328.
(4) De Rosa, C.; Auriemma, F. *Prog. Polym. Sci.* **2006**, *31*, 145–237.
(5) De Rosa, C.; Auriemma, F.; Corradi, M.; Caliano, L.; Talarico, G. *Macromolecules* **2008**, *41*, 8712–8720.
(6) Seguela, R. *J. Macromol. Sci. C. Polym. Rev.* **2005**, *45*, 263–287.
(7) Kakiage, M.; Yamanobe, T.; Komoto, T.; Murakami, S.; Uehara, H. *Polymer* **2006**, *47*, 8053–8060.
(8) Kawakami, D.; Ran, S.; Burger, C.; Fu, B.; Sics, I.; Chu, B.; Hsiao, B. S. *Macromolecules* **2003**, *36*, 9275–9280.
(9) Kawakami, D.; Ran, S.; Burger, C.; Avila-Orta, C.; Sics, I.; Chu, B.; Hsiao, B. S.; Kikutani, T. *Macromolecules* **2006**, *39*, 2909–2920.
(10) Kawakami, D.; Hsiao, B. S.; Burger, C.; Ran, S.; Avila-Orta, C.; Sics, I.; Kikutani, T.; Jacob, K. I.; Chu, B. *Macromolecules* **2005**, *38*, 91–103.
(11) Gorlier, E.; Haudin, J. M.; Billon, N. *Polymer* **2001**, *42*, 9541–9549.

(12) Welsh, G. E.; Blundell, D. J.; Windle, A. H. *Macromolecules* **1998**, *31*, 7562–7565.
(13) Welsh, G. E.; Blundell, D. J.; Windle, A. H. *J. Mater. Sci.* **2000**, *35*, 5225–5240.
(14) Bonart, R. *Kolloid-Z.* **1966**, *213*, 1–11.
(15) Jakeways, R.; Klein, J. L.; Ward, I. M. *Polymer* **1996**, *37*, 3761–3762.
(16) Mahendrasingam, A.; Martin, C.; Fuller, W.; Blundell, D. J.; Oldman, R. J.; MacKerron, D. H.; Harvie, J. L.; Riekel, C. *Polymer* **2000**, *41*, 1217–1221.
(17) Miri, V.; Persyn, O.; Lefebvre, J. M.; Seguela, R.; Stroeks, A. *Polymer* **2007**, *48*, 5080–5087.
(18) Samon, J. M.; Schultz, J. M.; Hsiao, B. S. *Polymer* **2000**, *41*, 2169–2182.
(19) Penel-Pierron, L.; Seguela, R.; Lefebvre, J.-M.; Miri, V.; Depecker, C.; Jutigny, M.; Pabiot, J. *J. Polym. Sci., Part B: Polym. Phys.* **2001**, *39*, 1224–1236.
(20) Northolt, M. G.; Tabor, B. J.; van Aartsen, J. *J. Polym. Sci., Part A-2: Polym Phys* **1972**, *10*, 191–192.
(21) Hiramatsu, N.; Haraguchi, K.; Hirakawa, S. *J. Appl. Phys.* **1983**, *22*, 335–339.
(22) Ishikawa, T.; Nagai, S.; Kasai, N. *Makromol. Chem.* **1981**, *182*, 977–988.
(23) Mathias, L. J.; Johnson, C. G. *Macromolecules* **1991**, *24*, 6114–6122.
(24) Ramesh, C. *Macromolecules* **1999**, *32*, 5704–5706.
(25) Li, L. B.; Koch, M. H. J.; de Jeu, W. H. *Macromolecules* **2003**, *36*, 1626–1632.
(26) Dencheva, N.; Nunes, T. G.; Oliveira, M. J.; Denchev, Z. *J. Polym. Sci., Part B: Polym. Phys.* **2005**, *43*, 3720–3733.
(27) Arimoto, H.; Ishibashi, M.; Hirai, M.; Chatani, Y. *J. Polym. Sci.* **1965**, *A3*, 317–326.
(28) Aharoni, S. M. *n-Nylons: Their Synthesis, Structure and Properties*; John Wiley & Sons: Chichester, U.K., 1997; Chapter 1.3
(29) Murthy, N. S. *J. Polym. Sci., Part B: Polym. Phys.* **2006**, *44*, 1763–1782.
(30) Song, J. B.; Zhang, H. L.; Ren, M. Q.; Chen, Q. Y.; Sun, X. H.; Wang, S. Y.; Zhang, H. F.; Mo, Z. S. *Macromol. Rapid Commun.* **2005**, *26*, 487–490.
(31) Bowden, P.; Young, R. *J. Mater. Sci.* **1974**, *9*, 2034–2051.
(32) Peterlin, A. *J. Mater. Sci.* **1971**, *6*, 490–508.
(33) Men, Y. F.; Rieger, J.; Strobl, G. *Phys. Rev. Lett.* **2003**, *91*, 095502.
(34) De Rosa, C.; Auriemma, F.; de Ballesteros, O. R. *Phys. Rev. Lett.* **2006**, *96*, 167801.
(35) Hiss, R.; Hobeika, S.; Lynn, C.; Strobl, G. *Macromolecules* **1999**, *32*, 4390–4403.
(36) Seguela, R.; Rietsch, F. *J. Mater. Sci. Lett.* **1990**, *9*, 46–47.
(37) Kiho, H.; Peterlin, A.; Geil., P. H. *J. Appl. Phys.* **1964**, *35*, 1599–1605.
(38) Butler, M. F.; Donald, A. M. *Macromolecules* **1998**, *31*, 6234–6249.
(39) Butler, M. F.; Donald, A. M.; Bras, W.; Mant, G. R.; Derbyshire, G. E.; Ryan, A. J. *Macromolecules* **1995**, *28*, 6383–6393.
(40) Schrauwen, B. A. G.; Janssen, R. P. M.; Govaert, L. E.; Meijer, H. E. H. *Macromolecules* **2004**, *37*, 6069–6078.
(41) Butler, M. F.; Donald, A. M. *Polymer* **1997**, *38*, 5521–5538.
(42) Butler, M. F.; Donald, A. M.; Ryan, A. J. *Polymer* **1998**, *39*, 39–52.
(43) Butler, M. F.; Donald, A. M.; Ryan, A. J. *Polymer* **1998**, *39*, 781–792.
(44) Bai, L. G.; Hong, Z. H.; Wang, D. L.; Li, J. J.; Wang, X.; Li, L. B. Submitted for publication in *Macromolecules*.
(45) Rhee, S.; White, J. L. *J. Polym. Sci., Part B: Polym. Phys.* **2002**, *40*, 1189–1200.
(46) Harumi, S.; Shigehiro, S.; Kimihiro, M.; Yasuo, K.; Hiroshi, Y.; Heinz, W. S.; Yukihiro, O. *Macromol. Chem. Phys.* **2003**, *204*, 1351–1358.
(47) Christopher, J. O.; Dale, L. H.; Bruce, C. B. *J. Phys. Chem. C* **2009**, *113*, 13723–13731.
(48) Hendra, P. J.; Maddams, W. F.; Royaud, I. A.; Willis, H. A.; Zichy, V. *Spectrochim. Acta, Part A* **1990**, *46*, 747–756.
(49) Orendorff, C. J.; Ducey, M. W.; Pemberton, J. E. *J. Phys. Chem. A.* **2002**, *106*, 6991–6998.
(50) Natta, G.; Corradini, P. *Nuovo Cim., Suppl.* **1960**, *15*, 40–51.